ORGANOMETALLICS

Article

Cite This: *Organometallics* XXXX, XXX, XXX−XXX

Conformational Control of Initiation Rate in Hoveyda−Grubbs Precatalysts

Zackary R. Gregg, Justin R. Griffiths, and Steven T. Diver*

Department of Chemistry, University at Buffalo, the State University of New York, Buffalo, New York 14260-3000, United States

Supporting Information

ABSTRACT: When the coordinating isopropyl ether of the Hoveyda precatalyst is replaced by a cyclohexyl ether, it is possible to control the substituent's conformation in either the equatorial or axial position. A stereodivergent synthesis of axial and equatorial cyclohexyl vinyl ethers provided access to new ruthenium metathesis precatalysts by carbene exchange. The conformational disposition of the coordinating aryl ether was found to have a significant effect on the reactivity of the precatalyst in alkene metathesis. The synthesis of four new Ru carbene complexes is reported, featuring either the 1,3-bis(2,4,6-trimethylphenyl)dihydroimidazolylidene (H_2IMes) or the 1,3-bis(2,6-diisopropylphenyl)-dihydroimidazolylidene (SIPr) N-heterocyclic carbene ligand. The conformational isomers in the SIPr series were structurally characterized. Performance testing of all new precatalysts in three different ring-closing metatheses and an alkene cross metathesis illustrated superior performance by the precatalysts bearing axial coordinating ethers. Initiation rates with butyl vinyl ether were also measured, providing a useful comparison to existing Hoveyda-type metathesis precatalysts. Use of conformational control of the coordinating ether substituent provides a new way to modulate reactivity in this important class of alkene metathesis precatalysts.

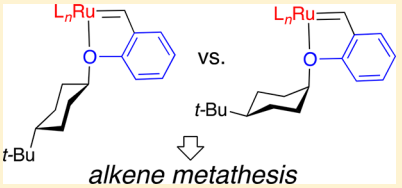

INTRODUCTION

New metathesis applications continue to drive the development of new ruthenium carbene initiators, known widely as Grubbs catalysts. A rapid initiation rate is critical for successful ring-opening polymerizations and for promoting ring-closing metathesis. In 1999, Hoveyda and co-workers[1] developed a chelated carbene catalyst, and shortly thereafter, the second-generation catalyst **Ru1** bearing a H_2IMes N-heterocyclic carbene (NHC) ligand was reported.[2] The chelating ether motif is extremely important and versatile, as it provides a platform to control initiation rate, an important determinant of metathesis activity. The parent complex **Ru1** is known as the Hoveyda or Hoveyda-Grubbs precatalyst, and other precatalysts that contain the chelating ether motif fall into a superfamily of metathesis initiators known as Hoveyda-type precatalysts.[3] Hoveyda-type initiators have been utilized in some of the most synthetically demanding metathesis applications in organic synthesis.[4]

The Hoveyda chelate design has allowed access to diverse precatalysts with different initiation profiles thereby suited to particular metathesis applications. In most cases, the chelated ruthenium carbene complex can be purified by column chromatography and often can be recrystallized. The benzene ring of the chelating ether can be modified to increase the initiation rate. For instance, the addition of an electron-withdrawing *p*-nitro group results in the electronically activated precatalyst **Ru2** known as the Grela catalyst[5] (Scheme 1). Other aromatic ring substituents also influence the initiation reaction rate and affect the mechanism of initiation, as shown by Plenio and co-workers.[6] Steric effects also result in an activated catalyst. An adjacent ring substituent can exert a steric

Scheme 1. Hoveyda-Type Catalysts with Different Initiation Rates

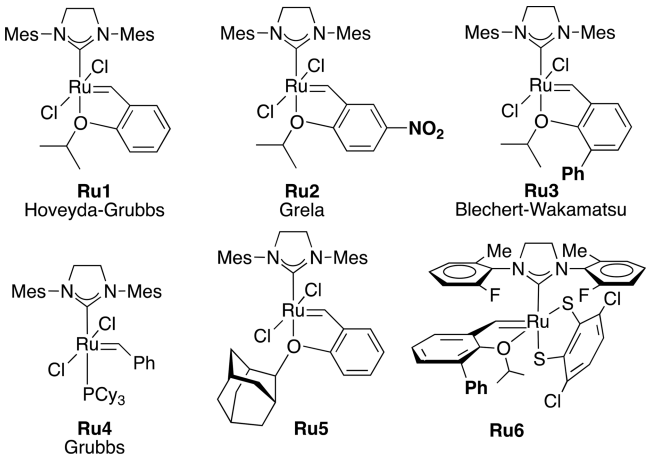

buttressing effect as in **Ru3**, forcing the isopropyl group into greater steric clash with the $RuCl_2$ fragment, leading to a dramatic increase in initiation rate.[7] If the isopropyl group of **Ru1** is replaced with an adamantyl group as in **Ru5**, there is a profound steric effect, destabilizing the chelate and increasing the initiation rate. Grubbs et al. showed this steric effect on metathesis through measurement of initiation rates with vinyl ethers.[8] Recently, Grubbs and Ahmed used the phenyl buttressing design of Blechert and Wakamatsu[7] in catecholdi-

Received: January 23, 2018

DOI: 10.1021/acs.organomet.8b00041
Organometallics XXXX, XXX, XXX−XXX

Scheme 2. Will Axial Disposition of the Chelating Ether Oxygen Increase Initiation Rate?

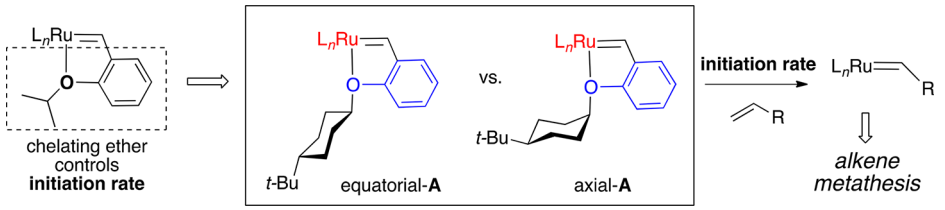

Scheme 3. Stereodivergent Synthesis of Conformers and Ru Carbene Catalysts

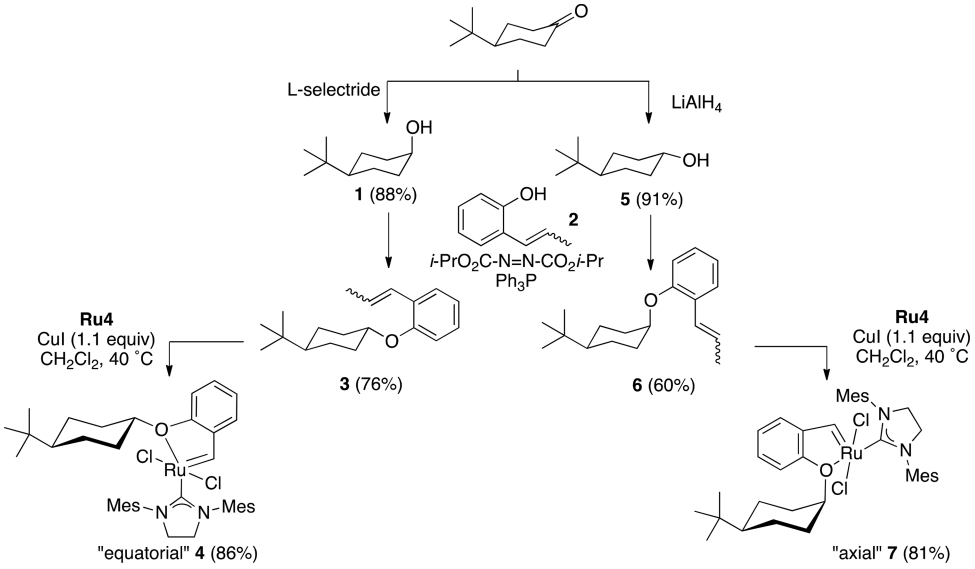

thiolate carbene **Ru6** complexes to make more reactive stereoretentive Ru carbene catalysts.[9] A more extensive discussion of all the modifications that have been made can be found in a review[10] and a recent book chapter.[11]

Despite this expansive set of ruthenium carbene precatalysts, to our knowledge, modulation of initiation rate has never been achieved by placing the coordinating ether in conformationally distinct positions in a chair cyclohexane ring. The arylidene containing the coordinating isopropyl ether is dislodged by an alkene in the initiation step.[12,6b] For some reactions, such as ring-closing metathesis (RCM) of diethyl diallylmalonate (DEDAM), the rate of initiation dictates the rate of alkene metathesis.[13,6a] By modification of the isopropyl group into a cyclohexyl group, the coordinating ether substituent can be either equatorial or axial. For simple substituents, such as an ether, the *A* value is about 0.8 kcal/mol, which means that the axial conformer is 0.8 kcal/mol higher in energy than the equatorial isomer due to destabilizing 1,3-diaxial interactions. In the coordinated ether substituent $-O(Ar)(RuL_n)$, the substituent is larger and likely has a larger *A* value, see axial-**A** in Scheme 2. We hypothesized that if the ether oxygen was held into an axial position such as in axial-**A** (Scheme 2), the greater conformational strain experienced by the $-O(Ar)(RuL_n)$ substituent would favor loss of the RuL_n group, resulting in a faster initiation rate. In this work, we validated this hypothesis by synthesizing new Hoveyda complexes bearing either axial or equatorial cyclohexyl aryl ethers. Performance testing in RCM and initiation studies with an alkyl vinyl ether showed that the axial conformer had increased metathesis activity. We utilized this knowledge to efficiently run challenging ring-closing and cross-metathesis reactions. We applied this new concept of conformationally controlled initiation activity to a different catalyst with a different NHC, the 1,3-bis(2,6-diisopropylphenyl)dihydroimidazolylidene (SIPr) ligand. This latter initiator proved highly effective for RCM reactions that form tetrasubstituted cycloalkenes and for cross alkene metathesis.

RESULTS AND DISCUSSION

Conformational control was achieved through a conformationally locked cyclohexane ring. To restrict the aryl ether to an axial or equatorial position, a *tert*-butyl group was attached at the 4-position, where it resides in the equatorial position due to its steric bulk. If the cyclohexane features trans-1,4-disubstitution, the oxygen will be forced equatorial as in equatorial-**A**. In the cis-1,4-disubstituted isomer axial-**A** (Scheme 2b), the ether oxygen is forced exclusively in the axial position. This expected steric strain will raise the energy of the cis diastereomer; loss of Ru from oxygen binding will reduce the *A* value of the cyclohexyl ether and lower the energy of Ru−O dissociation relative to the equatorial isomer. Initiation of the parent Hoveyda complex with small alkenes proceeds by an associative mechanism, leading to a higher energy alkene complex.[14a,b,6b,14c] The higher ground state energy of the axial-**A** conformer will result in a lower activation energy en route to the higher energy reactive intermediates in the initiation pathway. This thinking formed the basis for the design of the catalysts in this study.

The stereodivergent synthesis of the cis and trans isomers proceeded from a common commercially available starting material, 4-*tert*-butylcyclohexanone (Scheme 3). Equatorial hydride delivery with the bulky complex metal hydride L-

DOI: 10.1021/acs.organomet.8b00041
Organometallics XXXX, XXX, XXX−XXX

Selectride gave the axial alcohol **1** with high stereocontrol. A Mitsunobu reaction with phenol **2** gave the equatorial aryl ether **3** in 76% yield. Reaction of the Grubbs carbene **Ru4** with **3** in the presence of CuCl gave the equatorial catalyst **4** in good overall yield. The corresponding axial conformer (diastereomer) was produced by $LiAlH_4$ reduction to give **5** in a 9:1 diastereomeric ratio (equatorial:axial). A Mitsunobu reaction with phenol **2** was employed to install the axial ether, giving **6**. This was a more difficult reaction that resulted in lower yield and lower dr; however, pure diastereomer **6** was obtained after careful column chromatography. Carbene exchange by reaction of **6** with **Ru4** mediated by CuCl gave the axial conformer **7** in good yield. The carbene complexes **4** and **7** were purified by flash chromatography on silica gel, and the equatorial **4** was recrystallized by layering in dichloromethane–hexanes and allowing the mixture to stand at room temperature over several days in the glovebox.

With conformational isomers **4** and **7** in hand, we checked the rate of ring-closing metathesis of the simple diene, diethyl diallylmalonate (DEDAM) (eq 1). In terms of performance

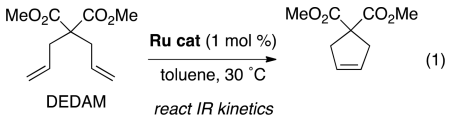

testing, this rate profile is commonly examined for new catalysts because the slowest step of this reaction is the initiation step.[15] Typically this reaction is monitored by in situ ^1H NMR, but we used in situ IR spectroscopy. In this way, the concentration of product was measured by observing the IR absorption at 1254 cm^{-1} for a C–O bond in the RCM product. The benchmark rate profile of the **Ru1** precatalyst was also determined and found to lie between the conformers **4** and **7** (Figure 1). The

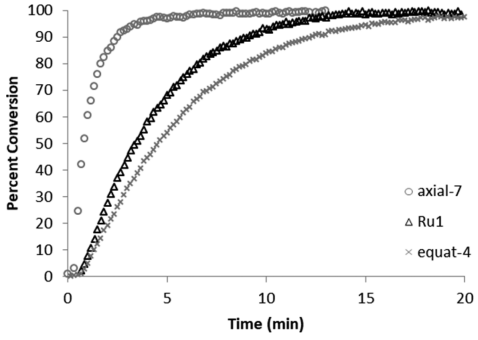

Figure 1. Percent conversion of diethyl diallylmalonate to its ring-closing metathesis product (eq 1), monitored by in situ IR versus time. Conditions: 0.05 M DEDAM, 0.5 mM Ru catalyst, toluene, 30 °C; reactant 1215 cm^{-1}, product, 1254 cm^{-1}.

equatorial isomer performed similarly to that of the **Ru1** complex, though slightly slower. In contrast, the axial precatalyst **7** promoted this reaction more quickly than **Ru1** and significantly more quickly than the equatorial isomer **4**. For the RCM of DEDAM, axial catalyst **7** was superior.

After observing a rate enhancement in the RCM of diethyl diallylmalonate for the axial catalyst, we wondered whether the same concept could be applied to a different Grubbs catalyst with a different N-heterocyclic carbene supporting ligand. Using the same axial and equatorial starting materials **3** and **6**, the CuCl-mediated carbene exchange reaction with the commercially available Grubbs catalyst **Ru7** produced two new diastereomeric precatalysts in excellent yield (Scheme 4). Precatalysts **8** and **9** bear a sterically hindered NHC, the 1,3-bis(2,6-diisopropylphenyl)dihyrdoimidazole (SIPr) ligand. As with the previous carbene complexes, these were purified by flash chromatography on silica gel. Recrystallization by dissolving in dichloromethane and layering with hexanes yielded X-ray-quality crystals.

The X-ray crystal structures were obtained for the axial and equatorial conformers of the SIPr carbene precatalysts. The equatorial Ru complex **8** is shown in Chart 1, and the axial Ru

Chart 1. X-ray Structure of Ru Carbene Complex 8 (Equatorial Aryl Ether)[a]

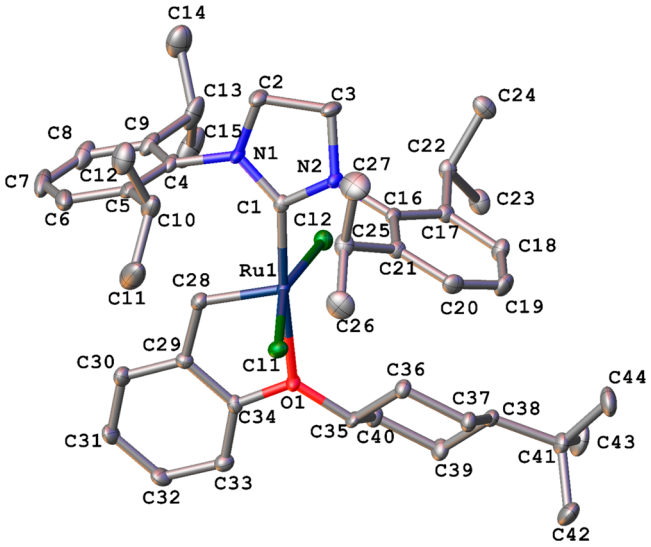

[a]Ellipsoids drawn at 50% probability. Hydrogen atoms have been omitted for clarity. Selected bond lengths: Ru–Cl1, 2.3343(9) Å; Ru–Cl2, 2.3445(9) Å; Ru–O1, 2.217(3) Å; Ru–C1, 1.966(4) Å; Ru–C28, 1.832(4) Å; O1–C35 1.470(4) Å.

complex **9** is shown in Chart 2. First, the solid-state structures confirm the equatorial and axial orientations of the aryl ether

Scheme 4. Synthesis of New Precatalysts Bearing a Different NHC Ligand

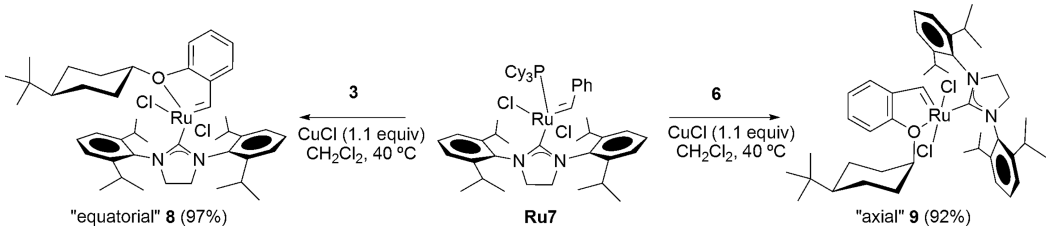

DOI: 10.1021/acs.organomet.8b00041
Organometallics XXXX, XXX, XXX–XXX

Chart 2. X-ray Structure of Ru Carbene Complex 9 (Axial Aryl Ether)[a]

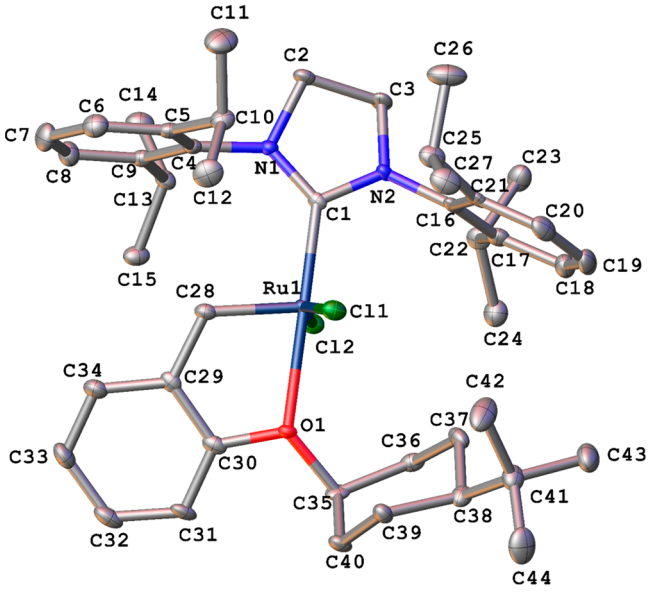

[a]Ellipsoids drawn at 50% probability. Hydrogen atoms have been omitted for clarity. Selected bond lengths: Ru−Cl1, 2.3199(4) Å; Ru−Cl2, 2.3396(5) Å; Ru−O1, 2.3118(13) Å; Ru−C1, 1.9736(17) Å; Ru−C28, 1.8181(19) Å, O1−C35, 1.477(2) Å.

substituent on the cyclohexane ring. Second, some bond length differences are consistent with greater steric strain in the axial conformer. Axial isomer **9** has a slightly longer Ru−O bond in the chelate: 2.3118(13) vs 2.217(3) Å for the equatorial isomer **8**. For comparison, the Ru−O bond length in the Grubbs 2-adamantyl complex **Ru5** is 2.338(3) Å.[8] The NHC ligand is slightly more distant from the Ru center in the axial isomer: 1.9736(17) vs 1.966(4) Å for the equatorial isomer. This may be due to the greater face strain between the Cl−Ru−Cl moiety and the cyclohexyl ether in the axial conformer. Finally, the equatorial ether substituent holds the chair cyclohexane ring closer to the aromatic ring of the NHC. For instance, the Ru−O1−C35 bond angle is 127.07°, whereas the same bond angle in the axial conformer is 131.16°. The axial conformer features a slightly greater separation of the cyclohexane ring and the aromatic ring of the N-heterocyclic carbene, which provides greater access to the Ru center by an approaching alkene. Other small structural differences are also noted, such as slightly longer Ru−Cl bonds in the equatorial isomer and a shorter Ru=C bond (Ru−C28) in the axial isomer. The difference in Ru−O bond length between the conformational isomers is most likely due to the steric strain imposed due to the conformation of the cyclohexyl ether; some of the smaller differences may result from additional interactions arising from crystal packing.[16]

When a more challenging diene substrate was used for the RCM reaction, performance testing for the new precatalysts revealed a significant difference in the equatorial and axial conformational isomers. A more challenging RCM may magnify catalyst differences, making it easier to compare them through reaction progress graphs (time−conversion plots). Ultimately, conversion data obtained from the Grubbs tests[17] helps compare new metathesis precatalysts with the available precatalysts; rate comparisons also aid catalyst selection for future synthetic applications. The reaction progress graph for the RCM shown in eq 2 is illustrated in Figure 2. A large number of data were obtained by in situ IR monitoring of the

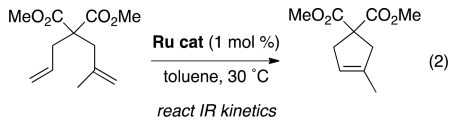

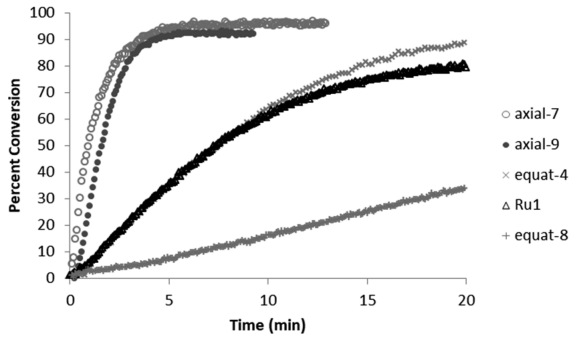

Figure 2. Conversion of dimethyl allyl(methylallyl)malonate to its ring-closing metathesis product, 4,4-dicarboethoxy-1-methylcyclopentene, monitored by in situ IR versus time. Conditions: 0.05 M diene, 0.5 mM Ru catalyst, toluene, 30 °C; reactant 1215 cm^{-1}, product, 1254 cm^{-1}.

reactant and product concentrations, by the distinctive C−O absorbances at 1215 and 1245 cm^{-1}, respectively. The rate profile of the **Ru1**-promoted reaction provides a reference for this ring-closing metathesis. As expected, the equatorial H_2IMes precatalyst **4** showed a rate profile almost identical with that of the **Ru1** precatalyst. The SIPr equatorial precatalyst **8** promoted this RCM at a much slower rate. Interestingly, both axial precatalysts **7** and **9** showed pronounced rates of catalysis for this transformation even though they have different initiation rates (see below).

Quantitative data such as the k_{obs} rate constants can be extracted from the reaction progress plots. By a plot of ln [diene] versus time, k_{obs} can be obtained as the slopes of the lines (see the Supporting Information for the plot), as summarized in Table 1. The rate constant for the Hoveyda

Table 1. Apparent Rate Constants (k_{obs}) for the RCM of Dimethyl Allyl(Methylallyl)Malonate[a]

entry	precatalyst	k_{obs} (10^{-3} s^{-1})[b]	k_{rel}[c]
1	**Ru1** (Hoveyda)	1.70	3.95
2	equatorial-**4**	2.09	4.86
3	axial-**7**	11.14	25.9
4	equatorial-**8**	0.432	1.00
5	axial-**9**	12.33	28.7

[a]Conditions: 0.05 M dimethyl allyl(methylallyl)malonate, 1 mol % catalyst loading, 30 °C. [b]k_{obs} is determined from the slope of the linear region after the induction period. [c]k_{rel} is based on **8** in entry 4.

complex **Ru1** provides a point of reference (entry 1). Each of the precatalysts **7** and **9** promoted this reaction about 7 times faster than **Ru1**. When equatorial is compared to axial (entry 2 vs 3; entry 4 vs 5), the axial conformer performed better. In the H_2IMes series, the rate difference for axial vs equatorial is a factor of 6; in the SIPr series, the rate difference is a factor of 28. The conformation of the ether ligand with respect to the cyclohexane ring affects the reaction rate. Interestingly, the axial SIPr precatalyst performed almost identically with the axial

DOI: 10.1021/acs.organomet.8b00041
Organometallics XXXX, XXX, XXX−XXX

H_2IMes precatalyst. A similar profile was previously observed by Nelson et al. for an SIPr catalyst in a comparative study of SIPr and H_2IMes-based Ru precatalysts.[18]

The new carbene precatalysts were evaluated for their performance in promoting a challenging RCM to form a tetrasubstituted cycloalkene (eq 3, Table 2). There are few

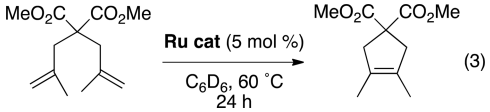

(3)

Table 2. Formation of a Tetrasubstituted Cycloalkene[a]

entry	precatalyst	yield (%)[b]
1	equatorial-**4**	59
2	axial-**7**	45
3	equatorial-**8**	40 (69)[c]
4	axial-**9**	82
5[d]	**Ru1** (Hoveyda)	30
6[e]	**Ru2** (Grela)	0

[a]Conditions: 0.1 M dimethyl bis(methylallyl)malonate, 5 mol % catalyst loading, C_6D_6, 60 °C, 24 h reaction time. [b]Average of two runs; determined by ^{1}H NMR spectroscopy. [c]After 91 h. [d]Taken from Grubbs et al.[19] [e]Taken from Grela et al.,[5] where the reaction was performed at 40 °C for 24 h.

catalysts that are proficient for this difficult RCM. We adopted the standard conditions used by Grubbs et al.,[19] who determined the conversion to product after 24 h at 60 °C. The yields are shown in Table 2. Surprisingly, the equatorial H_2IMes **4** proved superior to the axial conformer **7** (59% vs 47%, respectively). In comparison to the Hoveyda precatalyst **Ru1** (entry 5), all of the new precatalysts gave better yields. The shortcoming of the axial initiator **7** may be a result of rapid initiation, leading to a greater extent of catalyst decomposition. The results of the two conformers in the SIPr series showed the expected trend (entries 3 and 4): the equatorial **8** gave 40% yield, whereas the axial conformer **9** resulted in 82% yield after the standard reaction time. For this transformation, the structure of the catalyst's NHC ligand has a significant effect on the yield and a faster initiation rate alone is not adequate for the reaction of hindered diene substrates. To the best of our knowledge, the bis(1,3-diisopropylphenyl)-dihydroimidazolylidine ligand has not previously been shown to be a good NHC ligand for ring-closing metatheses that form tetrasubstituted cycloalkenes.[20]

The new precatalysts proved highly effective in promoting a difficult cross alkene metathesis. We adopted conditions similar to those reported by Grela, as shown in eq 4.[5] A 67% yield

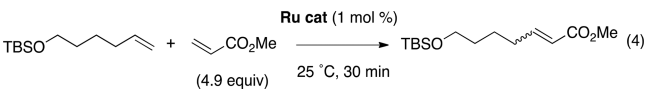

(4)

obtained with the Hoveyda precatalyst **Ru1** gives a baseline yield for comparison (entry 1, Table 3). The Grela precatalyst **Ru2** is highly proficient for this transformation, giving a 77% yield. A slight difference in the effectiveness of the conformers **4** and **7** was found (entries 3 and 4). The yield with the equatorial precatalyst was similar to that obtained with the Hoveyda precatalyst **Ru1**, and the yield obtained with the axial precatalyst was similar to that obtained with the Grela

Table 3. Results of Alkene Cross Metathesis Using New Precatalysts[a]

entry	precatalyst	yield (%)[b]	*E*:*Z* ratio
1	**Ru1** (Hoveyda)	67	>20:1
2	**Ru2** (Grela)	77	>20:1
3	equatorial-**4**	70	>20:1
4[c]	axial-**7**	75	>20:1
5	equatorial-**8**	66	3.8:1
6	axial-**9**	86	6.4:1
7	**Ru8**	69	4.7:1

[a]Conditions: 0.17 M **B** with 4.9 equiv of methyl acrylate in CH_2Cl_2, 1 mol % Ru cat, 25 °C, 30 min. [b]Yield determined by ^{1}H NMR vs mesitylene internal standard. [c]For this entry, yield and *E*:*Z* ratio represent the average of two runs.

precatalyst **Ru2**. In the SIPr series, the difference was more significant: 86% yield obtained with the axial conformer **9** was superior to the corresponding equatorial catalyst **8**, which gave 66% yield. The similarity of the performance of the axial H_2IMes precatalyst **7** to that displayed by the Grela precatalyst **Ru2** suggested that these carbene complexes may have similar initiation rates. On the basis of this suspicion, we investigated initiation rates next.

Finally, the initiation rate with butyl vinyl ether was measured (eq 5). We followed standard conditions so that

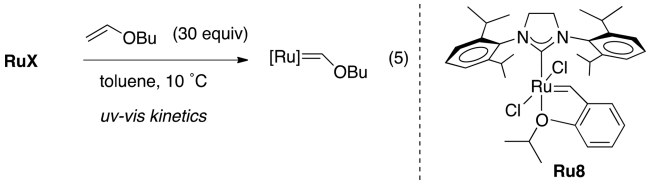

(5)

Table 4. Initiation Rates of New Precatalysts with Butyl Vinyl Ether[a]

entry	precatalyst	k_{obs}[b] (10^{-4} s^{-1})	k_{rel}[d]
2	equatorial-**4**	0.16 ± 0.05	9.41
2	axial-**7**	34 ± 2	2000
3[c]	equatorial-**8**	0.017 ± 0.004	1.00
4	axial-**9**	1.4 ± 0.2	82.4
5[c]	**Ru8**	0.022 ± 0.008	1.29

[a]Conditions: 10^{-4} M Ru-cat, 3×10^{-3} M butyl vinyl ether (BuVE), 10 °C, in distilled toluene, measured by absorbance at 380 nm by UV–vis. [b]k_{obs} is the average of three trials. k_{obs} was determined through the slope of $\ln(A_t - A_{inf}) - \ln(A_0 - A_{inf})$ vs time. [c]k_{obs} was determined from the linear region of ln [catalyst] vs time, and [catalyst] was determined through the Beer–Lambert law. [d]k_{rel} is equal to $k_{obs}/(k_{obs}$ of **8**).

we could make comparisons to known Hoveyda-type precatalysts. We monitored the disappearance of the Ru precatalyst by measuring the absorbance at 380 nm, which gave k_{obs} under pseudo-first-order conditions.[8] Similarly to the data obtained above, the equatorial and axial precatalysts showed significant differences in the initiation rates (Table 4). In entry 1, the equatorial precatalyst **4** registered a k_{obs} value similar to the reported literature value for the Hoveyda complex **Ru1**.[8] The axial precatalyst **7** registered a k_{rel} value of 2000 (entry 2). On comparison of the equatorial and axial conformers (entries 1 and 2), the axial precatalyst **7** reacted >200 times faster than **4**. In the SIPr series, equatorial **8** was the slowest initiator with a k_{rel} value of 1.00 (entry 3), whereas the

DOI: 10.1021/acs.organomet.8b00041
Organometallics XXXX, XXX, XXX–XXX

axial precatalyst **9** reacted 82 times faster (entry 4). In the SIPr series, comparison was made to a commercially available catalyst, **Ru8**. As expected, **Ru8** showed a rate similar to that for equatorial **8**. On comparison of the equatorial conformers in entries 1 and 3, it is not surprising that the equatorial H_2IMes precatalyst **4** is a faster initiator. The mechanism for initiation with small alkenes such as butyl vinyl ether are associative and bimolecular; the greater steric bulk of the 2,6-diisopropyl substitution of **8** impedes alkene association, resulting in a slower initiation rate. However, the greater steric bulk of the NHC ligand alone does not control the initiation rate: SIPr-based **9** reacts about 9 times faster than H_2IMes-based **4** (82.4 vs 9.41, entries 4 and 1, respectively).

Comparison to other Hoveyda-type precatalysts was possible, giving a direct measure of the effectiveness of the arylidene linker in the initiation step of alkene metathesis. For instance, literature data show that **Ru1** has $k_{obs} = 0.401 \times 10^{-4}$ s^{-1} and **Ru2** (Grela precatalyst) has $k_{obs} = 0.757 \times 10^{-4}$ s^{-1}, giving a k_{rel} value of 23.6 for **Ru1** and k_{rel} value of 44.5 for **Ru2**. This comparison, on the basis of separate measurements made by Grubbs et al.[8] and ourselves under identical conditions, illustrates that the fastest initiating new axial precatalyst **7** is about 84 times more reactive than **Ru1** and 45 times more reactive than **Ru2**. In addition, comparison to Grubbs' 2-adamantyl precatalyst **Ru5** is possible. The 2-adamantyl precatalyst **Ru5** has its aryl ether locked into an axial position; k_{obs} was determined to be 54.4×10^{-4} s^{-1},[8] which would give a k_{rel} value of 3200 (based on **8**) in comparison to the set of precatalysts in Table 4. **Ru5** is a faster initiator than axial **7** by a factor of 1.5. **Ru5** and axial **7** should have similar rates of initiation, but small differences in ring strain and rotamer population may account for the observed difference between these two initiation rates.

CONCLUSION

In summary, we synthesized four new Ru carbene complexes that bear arylidene ethers in conformationally distinct positions on a cyclohexane ring. The conformation of the aryl ether was found to affect the reactivity of the new precatalysts. A simple stereodivergent synthesis starting from commercially available 4-*tert*-butylcyclohexanone provided access to the equatorial and axial conformers. The modular nature of the synthesis allows for conformationally disposed ethers to be installed in different Grubbs catalyst environments, such as those bearing different N-heterocyclic carbene ligands. The axial or equatorial conformation of the coordinated ether was found to have a significant influence on the rate of ring-closing metathesis and on the initiation rate. In three different ring-closing metatheses, in an alkene cross metathesis, and in reaction with butyl vinyl ether, the precatalysts with the axially disposed aryl ether performed better than the corresponding equatorial conformers. Solid-state structures for the conformational isomers in the SIPr series both confirmed the structure and showed differences in the Ru−O bond length. Interestingly, the SIPr catalysts performed well for the synthesis of tetrasubstituted cycloalkenes and the axial SIPr catalyst proved to be superior for a cross alkene metathesis. In the axial position, the Ru-coordinated aryl ether has a higher steric strain which is partially alleviated upon decoordination of the Ru atom, leading to a lower activation energy for the initiation step. Overall, the conformation of the aryl ether was found to be an important determinant affecting alkene metathesis reactivity of different Hoveyda-type catalysts. Use of a defined conformation to improve the initiation rate may prove useful for challenging cross alkene metathesis applications. Future catalyst design using conformational control of the ether substituent is foreseeable.

EXPERIMENTAL SECTION

General Considerations. Unless otherwise stated, all reactions were performed using standard Schlenk line techniques under nitrogen with oven or flame-dried glassware. Solvents used in reactions were obtained from an anhydrous column purification system. Grubbs carbenes were obtained from Materia Inc. (Pasadena, CA) and used as received. Commercially available reagents were used as received unless otherwise noted. Diethyl diallylmalonate, butyl vinyl ether, methyl acrylate, and benzene-d_6 were distilled before use. Copper(I) chloride was recrystallized from concentrated hydrochloric acid, washed with deionized water, and dried in vacuo. Flash chromatography was carried out on untreated silica gel 60 from Sorbtech Technologies Inc. (230−400 mesh) under air pressure. Thin-layer chromatography (TLC) was performed on glass-backed silica plates (F254, 250 μm thickness, EMD Millipore), visualized with UV light, phosphomolybdic acid, iodine, or potassium permanganate. IR kinetics were obtained using a ReactIR iC10 instrument equipped with a K4 conduit and a SiComp sensor (2.5 cm × 10 cm) running iC IR software. ^{1}H NMR spectra were recorded at 300, 400, or 500 MHz; proton-decoupled ^{13}C NMR spectra were recorded at 75, 101, or 125 MHz using Varian Mercury 300, Inova 400, and Inova 500 instruments, and proton-decoupled ^{31}P NMR spectra were recorded at 121 MHz on a Varian Inova 400 spectometer. ^{1}H NMR chemical shifts are reported in ppm relative to the solvent used (chloroform-*d*, ^{1}H 7.26 ppm, ^{13}C 77 ppm; benzene-d_6, ^{1}H 7.15 ppm, ^{13}C 128.06 ppm; dichloromethane-d_2, ^{1}H 5.32 ppm), and ^{31}P was referenced using H_3PO_4 as an external reference. Infrared spectra were recorded using a PerkinElmer Spectrum Two FTIR-ATR instrument. Mass analysis was performed on a Bruker SolariX 12T FTMS apparatus using electrospray ionization with acetonitrile or dichloromethane as solvent. UV−vis studies were performed using a Cary 3E or a Cary 300 Bio UV−visible spectrometer, with temperature control. Computer-generated first-order fits were performed using the Cary WinUV kinetics software.

Preparation of 6. In a flame-dried 50 mL round-bottom flask equipped with magnetic stirbar were successively placed triphenylphosphine (1.10 g, 4.2 mmol), 4-*trans*-*tert*-butylcyclohexanol (984.7 mg, 6.3 mmol), **2** (282.4 mg, 2.1 mmol), triethylamine (580 μL, 4.2 mmol), and THF (7.05 mL). The reaction mixture was then stirred at room temperature for 1 h. The solution was cooled to 0 °C, and then diisopropyl azodicarboxylate (820 μL, 4.2 mmol) was added dropwise, allowing the orange color to dissipate between drops. The reaction mixture was maintained at 0 °C for 2 h then warmed to room temperature and stirred overnight. The mixture was concentrated by rotary evaporation and triturated with CH_2Cl_2 and hexanes to afford a colorless oil. Flash chromatography (0−20% gradient ethyl acetate−hexanes) afforded **6** (344 mg, 60%, >95% *Z*, and a single diastereomer by ^{1}H NMR) as a colorless oil. Analytical TLC: R_f 0.6 (10% EtOAc−hexanes); ^{1}H NMR (400 MHz, $CDCl_3$, ppm): δ 7.28 (d, ^3J = 7.2 Hz, 1 H, aromatic), 7.17 (t, ^3J = 8.4, 1 H, aromatic), 6.90 (t, ^3J = 7.8 Hz, 2 H, aromatic), 6.60 (d, ^3J = 11.1 Hz, 1 H, α-vinylic), 5.79 (dq, ^3J = 15.4 Hz, ^3J = 9.4 Hz, 1 H, β-vinylic), 4.58 (s, 1 H, C*H*OAr), 2.19−2.01 (m, 2 H, cyclohexyl), 1.84 (d, ^3J = 6.9 Hz, 3 H, CH_3), 1.58−1.38 (m, 6 H, cyclohexyl), 1.11−0.95 (m, 1 H, cyclohexyl), 0.87 (s, 9 H, *tert*-butyl). ^{13}C{^{1}H} NMR (75 MHz, $CDCl_3$, ppm): δ 154.95, 130.28, 127.86, 127.60, 126.10, 125.69, 119.68, 113.89, 71.28, 47.64, 32.57, 30.19, 27.48, 21.37, 14.73. FT-IR (ATR, cm^{-1}): 3024, 2940, 2866, 1596, 1483, 1449, 1393, 1365, 1285, 1230, 1177, 1111, 1032, 1005, 962, 928, 853, 749, 699. High-resolution MS (EI$^+$, m/z): molecular ion calculated for $C_{19}H_{28}O$ [M$^+$] 272.2135, found 272.2137, error 0.9 ppm.

Preparation of 3. In a 50 mL Schlenk tube containing a magnetic stirbar were placed 650 mg of cyclohexanol **1** (4.15 mmol, 3 equiv), 186 mg of *Z*-**2** (1.39 mmol, 1.00 equiv), 729 mg of triphenylphosphine (2.78 mmol, 2 equiv), 0.39 mL of triethylamine (0.28 g, 2.78 mmol,

DOI: 10.1021/acs.organomet.8b00041
Organometallics XXXX, XXX, XXX−XXX

2.0 equiv), and 5 mL of THF. The solution was cooled to 0 °C, whereupon 0.55 mL of diisopropylazodicarboxylate (0.56 g, 2.78 mmol, 2 equiv) was added dropwise via microliter syringe. After 2.5 h, TLC indicated complete consumption of the limiting reagent. The crude reaction mixture was concentrated in vacuo (rotary evaporator) and dissolved in ca. 0.5 mL of CH_2Cl_2, and the solids were crashed out by addition of 50 mL of hexanes. After the filtrate was decanted, the process was repeated, keeping the filtrate and evaporating solvents. The crude product was purified by flash chromatography (gradient elution 0−10% ethyl acetate−hexanes) to give 287 mg of *Z*-**3** (76%). Analytical TLC: R_f 0.6 (10% ethyl acetate−hexanes). ^{1}H NMR ($CDCl_3$, 300 MHz, ppm): δ 7.30−7.26 (m, 1H, aromatic), 7.17 (t, ^3J = 7.5 Hz, 1H, aromatic), 6.93−6.89 (m, 2H, aromatic), 6.54 (d, $^3J_{cis}$ = 11.1 Hz, 1H, α-vinyl), 5.79 (dq, $^3J_{cis}$ = 11.1, ^3J = 7.2 Hz, 1H, β-vinyl), 4.12−4.02 (m, 1H, C*H*OAr), 2.18 (br d, ^3J = 12.3 Hz, 2H, cyclohexyl), 1.86−1.82 (m, 5H, methyl and cyclohexyl), 1.48−1.36 (m, 2H, cyclohexyl), 1.16−1.08 (m, 3H, cyclohexyl), 0.87 (s, 9H, *tert*-butyl). ^{13}C NMR (75 MHz, CD_2Cl_2, ppm): δ 155.60, 130.25, 127.79, 127.63, 126.24, 125.58, 120.01, 114.49, 77.79, 47.32, 32.60, 32.31, 27.63, 25.57, 14.75. FT-IR (ATR, cm^{-1}): 2941, 2862, 1597, 1576, 1482, 1449, 1365, 1286, 1229, 1159, 1105, 1048, 1029, 982, 928, 901, 834, 748, 699. HR-MS (ESI): [M + Na$^+$] calcd for $C_{19}H_{28}O$ 295.2032, found 295.2032, error 0.1 ppm.

General Procedure for the Synthesis of Ruthenium Carbene Complexes. In the glovebox, a 50 mL Schlenk flask equipped with a magnetic stirbar was charged with Grubbs catalyst **Ru4** or **Ru7** (0.205 mmol, 1 equiv) and copper(I) chloride (22.3 mg, 0.226 mmol, 1.1 equiv). The flask was sealed, removed from the glovebox, placed under argon, and then the solids were dissolved in CH_2Cl_2 (16.4 mL). The corresponding styrenyl ether (0.24 mmol, 1.9 equiv) was injected, and the resulting solution was stirred at 40 °C or room temperature until complete consumption of the phosphine-containing precatalyst was observed by TLC (50% CH_2Cl_2−hexanes). Upon reaction completion, the reaction was concentrated in vacuo (rotary evaporator), and the resulting dark solid was purified by column chromatography (30−70% CH_2Cl_2−hexanes) to obtain the desired precatalyst as a green solid. Ru carbene complexes **4**, **8**, and **9** were recrystallized by slow diffusion of CH_2Cl_2 and hexanes in the glovebox over the course of several days.

Equatorial ***4***. Following the general procedure and using **Ru4** (50 mg, 0.059 mmol, 1.00 equiv), CuCl (6.4 mg, 0.065 mmol, 1.1 equiv), and *Z*-**3** (0.115 mmol, 1.95 equiv) for the reaction, 30.1 mg of **4** (71% yield) was isolated as a green solid. Analytical TLC: R_f 0.24 (50% CH_2Cl_2−pentane). ^{1}H NMR (400 MHz, $CDCl_3$, ppm): δ 16.54 (s, 1H, Ru=C*H*Ar), 7.46 (t, ^3J = 7.6 Hz, 1 H, aromatic), 7.07 (s, 4 H, mesityl aromatic C*H*), 6.92 (d, ^3J = 7.2 Hz, 1 H, aromatic), 6.84 (t, ^3J = 7.2 Hz, 1 H, aromatic), 6.78 (d, ^3J = 8.8 Hz, 1 H, aromatic), 4.51−4.43 (m, 1 H, C*H*OAr), 4.18 (s, 4 H, −CH_2CH_2−), 2.66−2.22 (br m, 18H, mesityl CH_3), 2.16 (d, ^3J = 11.6 Hz, 2 H, cyclohexyl), 1.75−1.63 (m, 2 H, cyclohexyl), 1.51−1.38 (m, 2 H, cyclohexyl), 1.01−0.91 (m, 3 H, cyclohexyl), 0.86 (s, 9 H, *tert*-butyl). ^{13}C{^{1}H} NMR (75 MHz, CD_2Cl_2, ppm): δ 296.67, 211.40, 152.42, 145.47, 139.15 (br, 2 C), 129.60, 129.57 (2C), 122.60, 122.41, 113.12, 81.63, 51.83, 47.16, 32.51, 31.42, 27.71, 25.89, 21.33, 19.68. FT-IR (ATR, cm^{-1}): 2950, 1587, 1438, 1453, 1395, 1259, 1217, 1016, 967, 913, 850, 744. HR-MS (FT-ICR ESI): $C_{38}H_{50}ON_2Cl_2Ru$, calcd for [M + Na$^+$] 745.2236, found 745.2265, error 3.9 ppm.

Axial ***7***. Following the general procedure and using **Ru4** (174.0 mg, 0.205 mmol), CuCl (22.3 mg, 0.226 mmol), and **6** (109.0 mg, 0.4 mmol) for the reaction, 119.5 mg of **7** (81% yield) was isolated as a green solid. Analytical TLC: R_f 0.13 (50% CH_2Cl_2−pentanes); R_f 0.63 (100% CH_2Cl_2). ^{1}H NMR (400 MHz, 323 K, C_6D_6, ppm): δ 16.84 (s, 1H, Ru=C*H*Ar), 7.16 (m, 1 H), 7.08 (dd, ^3J = 7.2 Hz, ^4J = 1.2 Hz, 1 H, aromatic), 7.00−6.90 (br s, 4 H, mesityl aromatic), 6.68 (t, ^3J = 10.4 Hz, 1 H, aromatic), 6.51 (d, ^3J = 8.4 Hz, 1 H, aromatic), 4.57−4.49 (m, 1 H, C*H*OAr), 3.46 (s, 4 H, −CH_2CH_2−), 2.80−2.40 (m, 12 H, mesityl *o*−CH_3), 2.28 (s, 6 H, mesityl *p*-CH_3), 1.77 (q, ^3J = 10 Hz, 2 H, cyclohexyl), 1.43−1.26 (m, 3 H, cyclohexyl), 1.25−1.15 (m, 2H, cyclohexyl), 1.01 (s, 9 H, *tert*-butyl), 0.79−0.88 (m, 3 H, cyclohexyl). ^{13}C{^{1}H} NMR (75 MHz, C_6D_6, ppm): δ 294.43, 212.06, 154.40, 146.34, 139.05, 135.88, 130.55, 129.97, 128.94, 128.62, 128.30, 123.28, 122.75, 114.70, 79.22, 51.96, 48.74, 33.59, 30.80, 30.51, 28.99, 28.21, 22.36, 21.83, 19.17. FT-IR (ATR, cm^{-1}): 2932, 2858, 2230, 1726, 1585, 1576, 1478, 1451, 1419, 1398, 1381, 1336, 1293, 1262, 1211, 1181, 1156, 1111, 1035, 1002, 915, 873, 852, 834, 780, 732, 645, 591, 580. High-resolution MS (ESI$^+$, *m*/*z*): molecular ion calculated for $C_{38}H_{50}Cl_2N_2ORu$ [M + formate] 767.2320, found 768.2361, error 6.2 ppm.

Equatorial ***8***. Following the general procedure and using **Ru7** (115.7 mg, 0.124 mmol), CuCl (13.9 mg, 0.14 mmol), and **6** (65.4 mg, 0.24 mmol) for the reaction, 97.0 mg of **8** (97% yield) was isolated as a green solid. Analytical TLC: R_f 0.42 (50% CH_2Cl_2−hexanes). ^{1}H NMR (323 K, 400 MHz, $CDCl_3$, ppm): δ 16.57 (s, 1 H, Ru=C*H*Ar), 7.41 (t, ^3J = 7.8 Hz, 2 H, aromatic), 7.31 (d, ^3J = 7.6 Hz, 4 H, aromatic), 7.17−7.10 (m, 1 H, aromatic), 7.04 (dd, ^3J = 7.6 Hz, ^4J = 1.6 Hz, 1 H, aromatic), 6.63 (t, ^3J = 7.6 Hz, 1 H, aromatic), 6.48 (d, ^3J = 8.4 Hz, 1 H, aromatic), 4.29−4.18 (m, 1 H, C*H*OAr), 3.87 (br s, 4 H, −CH_2CH_2−), 3.84 (sept, ^3J = 6.8 Hz, isopropyl C*H*), 2.26 (d, ^3J = 10.4 Hz, 2 H, cyclohexyl), 1.87 (q, ^3J = 12.4 Hz, 2 H, cyclohexyl), 1.59 (d, ^3J = 12.8, 2 H, cyclohexyl), 1.43 (d, ^3J = 5.2 Hz, 12 H, CH_3), 1.19 (d, ^3J = 6.8 Hz, 12 H, CH_3), 0.96 (t, ^3J = 12 Hz, 1 H, cyclohexyl), 0.79 (s, 9 H, *tert*-butyl), 0.76−0.62 (q, ^3J = 14.8 Hz, 2 H, cyclohexyl). ^{13}C NMR (323 K, 101 MHz, C_6D_6, ppm): δ 288.88, 216.56, 153.74, 150.52, 145.65, 138.07, 130.48, 129.57, 125.20, 122.94, 122.84, 113.75, 81.90, 55.40, 53.90, 47.66, 32.80, 32.35, 29.85, 28.30, 27.41, 26.46, 24.31. FT-IR (ATR, cm^{-1}): 2945, 1586, 1472, 1452, 1408, 1387, 1296, 1263, 1234, 1219, 1109, 1010, 964, 866, 801, 757, 744. HR-MS (FT-ICR ESI): $C_{44}H_{62}ON_2Cl_2Ru$, calcd for [M$^+$] 806.3277, found 806.3280, error 0.4 ppm.

Axial ***9***. Following the general procedure and using **Ru7** (115.7 mg, 0.124 mmol), CuCl (13.9 mg, 0.14 mmol), and **6** (65.4 mg, 0.24 mmol) for the reaction, 91.7 mg of **9** (92% yield) was isolated as a green solid. Analytical TLC: R_f 0.4 (50% CH_2Cl_2−hexanes). ^{1}H NMR (323 K, 400 MHz, C_6D_6, ppm): δ 16.69 (s, 1 H, Ru = C*H*Ar), 7.40 (t, ^3J = 7.6 Hz, 2 H, aromatic), 7.29 (d, ^3J = 7.6 Hz, 4 H, aromatic), 7.11 (t, ^3J = 7.8 Hz, 1 H, aromatic), 6.98 (d, ^3J = 7.6 Hz, 1 H, aromatic), 6.62 (t, ^3J = 7.6 Hz, 1 H, aromatic), 6.48 (d, ^3J = 8.4, 1 H, aromatic), 4.56−4.50 (m, 1 H, C*H*OAr), 3.89−3.77 (m, 8 H, isopropyl C*H*, −CH_2CH_2−), 2.59 (dd, ^3J = 14.4 Hz, ^4J = 3.2 Hz, 2 H, cyclohexyl), 1.67 (q, ^3J = 12 Hz, 2 H, cyclohexyl), 1.46−1.31 (m, 14 H, 4CH_3, cyclohexyl), 1.22−1.14 (m, 14 H, 4CH_3, cyclohexyl), 0.89 (s, 9 H, *tert*-butyl), 0.85−0.77 (m, 1 H, cyclohexyl). ^{13}C{^{1}H} NMR (323 K, 101 MHz, C_6D_6, ppm): δ 289.61, 215.13, 154.60, 150.02, 145.30, 138.26, 130.75, 130.01, 125.49, 123.38, 122.80, 114.54, 114.27, 79.43, 55.55, 53.91, 48.41, 33.48, 30.52, 29.74, 28.99, 28.22, 27.23, 24.50, 22.38. FT-IR (ATR, cm^{-1}): 2964, 2867, 2280, 1585, 1475, 1453, 1440, 1409, 1386, 1362, 1326, 1297, 1260, 1232, 1211, 1181, 1157, 1111, 1049, 1002, 928, 874, 835, 803, 746. HR-MS (FT-ICR ESI): $C_{44}H_{62}ON_2Cl_2Ru$, calcd for [M$^+$] 806.3277, found 806.3289, error −0.7 ppm.

■ ASSOCIATED CONTENT

Supporting Information

The Supporting Information is available free of charge on the ACS Publications website at DOI: 10.1021/acs.organomet.8b00041.

Preparation of organic starting materials, procedure for kinetic monitoring of RCM reactions, procedure for cross alkene metathesis, and initiation procedure using the alkene butyl vinyl ether (PDF)

Accession Codes

CCDC 1828210−1828211 contain the supplementary crystallographic data for this paper. These data can be obtained free of charge via www.ccdc.cam.ac.uk/data_request/cif, or by emailing data_request@ccdc.cam.ac.uk, or by contacting The Cambridge Crystallographic Data Centre, 12 Union Road, Cambridge CB2 1EZ, UK; fax: +44 1223 336033.

DOI: 10.1021/acs.organomet.8b00041
Organometallics XXXX, XXX, XXX−XXX

AUTHOR INFORMATION

Corresponding Author

*E-mail for S.T.D.: diver@buffalo.edu.

ORCID

Steven T. Diver: 0000-0003-2840-6726

Notes

The authors declare no competing financial interest.

ACKNOWLEDGMENTS

This work was supported by the NSF (CHE-1300702). The authors thank Eric Sylvester and Prof. Jason Benedict for solving the crystal structures of **8** and **9** and Prof. Jerry Keister for helpful discussions. We gratefully acknowledge Materia, Inc. (Pasadena, CA), for supplying the Grubbs catalysts used in this work.

REFERENCES

(1) Kingsbury, J. S.; Harrity, J. P. A.; Bonitatebus, P. J.; Hoveyda, A. H. A Recyclable Ru-Based Metathesis Catalyst. *J. Am. Chem. Soc.* **1999**, *121*, 791−799.

(2) (a) Garber, S. B.; Kingsbury, J. S.; Gray, B. L.; Hoveyda, A. H. Efficient and Recyclable Monomeric and Dendritic Ru-Based Metathesis Catalysts. *J. Am. Chem. Soc.* **2000**, *122*, 8168−8179. (b) Gessler, S.; Randl, S.; Blechert, S. Synthesis and metathesis reactions of a phosphine-free dihydroimidazole carbene ruthenium complex. *Tetrahedron Lett.* **2000**, *41*, 9973−9976.

(3) Throughout this paper metathesis initiators are called "precatalysts". Upon intiation with an alkene, they give rise to the active carbene catalyst.

(4) (a) White, D. E.; Stewart, I. C.; Grubbs, R. H.; Stoltz, B. M. The Catalytic Asymmetric Total Synthesis of Elatol. *J. Am. Chem. Soc.* **2008**, *130*, 810−811. (b) Jackson, K. L.; Henderson, J. A.; Motoyoshi, H.; Phillips, A. J. A Total Synthesis of Norhalichondrin B. *Angew. Chem., Int. Ed.* **2009**, *48*, 2346−2350. (c) Dieckmann, M.; Kretschmer, M.; Li, P.; Rudolph, S.; Herkommer, D.; Menche, D. Total Synthesis of Rhizopodin. *Angew. Chem., Int. Ed.* **2012**, *51*, 5667−5670. (d) Ohyoshi, T.; Funakubo, S.; Miyazawa, Y.; Niida, K.; Hayakawa, I.; Kigoshi, H. Total Synthesis of (−)-13-Oxyingenol and its Natural Derivative. *Angew. Chem., Int. Ed.* **2012**, *51*, 4972−4975. (e) Gao, X.; Woo, S. K.; Krische, M. J. Total Synthesis of 6-Deoxyerythronolide B via C−C Bond-Forming Transfer Hydrogenation. *J. Am. Chem. Soc.* **2013**, *135*, 4223−4226. (f) Mewald, M.; Medley, J. W.; Movassaghi, M. Concise and Enantioselective Total Synthesis of (−)-Mehranine, (−)-Methylenebismehranine, and Related Aspidosperma Alkaloids. *Angew. Chem., Int. Ed.* **2014**, *53*, 11634−11639. (g) Wang, H.; Reisman, S. E. Enantioselective Total Synthesis of (−)-Lansai B and (+)-Nocardioazines A and B. *Angew. Chem., Int. Ed.* **2014**, *53*, 6206−6210. (h) Glaus, F.; Altmann, K.-H. Total Synthesis of the Tiacumicin B (Lipiarmycin A3/Fidaxomicin) Aglycone. *Angew. Chem., Int. Ed.* **2015**, *54*, 1937−1940. (i) Harvey, R. S.; Mackay, E. G.; Roger, L.; Paddon-Row, M. N.; Sherburn, M. S.; Lawrence, A. L. Total Synthesis of Ramonanins A−D. *Angew. Chem., Int. Ed.* **2015**, *54*, 1795−1798. (j) Jecs, E.; Diver, S. T. Two Ene−Yne Metathesis Approaches to the Total Synthesis of Amphidinolide P. *Org. Lett.* **2015**, *17*, 3510−3513. (k) Kita, M.; Oka, H.; Usui, A.; Ishitsuka, T.; Mogi, Y.; Watanabe, H.; Tsunoda, M.; Kigoshi, H. Total Synthesis of Mycalolides A and B through Olefin Metathesis. *Angew. Chem., Int. Ed.* **2015**, *54*, 14174−14178. (l) Korch, K. M.; Eidamshaus, C.; Behenna, D. C.; Nam, S.; Horne, D.; Stoltz, B. M. Enantioselective Synthesis of α-Secondary and α-Tertiary Piperazin-2-ones and Piperazines by Catalytic Asymmetric Allylic Alkylation. *Angew. Chem., Int. Ed.* **2015**, *54*, 179−183. (m) Švenda, J.; Sheremet, M.; Kremer, L.; Maier, L.; Bauer, J. O.; Strohmann, C.; Ziegler, S.; Kumar, K.; Waldmann, H. Biology-Oriented Synthesis of a Withanolide-Inspired Compound Collection Reveals Novel Modulators of Hedgehog Signaling. *Angew. Chem., Int. Ed.* **2015**, *54*, 5596−5602.

(5) Grela, K.; Harutyunyan, S.; Michrowska, A. A highly efficient ruthenium catalyst for metathesis reactions. *Angew. Chem., Int. Ed.* **2002**, *41*, 4038−4040.

(6) (a) Vorfalt, T.; Wannowius, K.-J.; Plenio, H. Probing the Mechanism of Olefin Metathesis in Grubbs−Hoveyda and Grela Type Complexes. *Angew. Chem., Int. Ed.* **2010**, *49*, 5533−5536. (b) Thiel, V.; Hendann, M.; Wannowius, K.-J.; Plenio, H. On the Mechanism of the Initiation Reaction in Grubbs-Hoveyda Complexes. *J. Am. Chem. Soc.* **2012**, *134*, 1104−1114.

(7) Wakamatsu, H.; Blechert, S. A New Highly Efficient Ruthenium Metathesis Catalyst. *Angew. Chem., Int. Ed.* **2002**, *41*, 2403−2405.

(8) Engle, K. M.; Lu, G.; Luo, S.-X.; Henling, L. M.; Takase, M. K.; Liu, P.; Houk, K. N.; Grubbs, R. H. Origins of Initiation Rate Differences in Ruthenium Olefin Metathesis Catalysts Containing Chelating Benzylidenes. *J. Am. Chem. Soc.* **2015**, *137*, 5782−5792.

(9) Ahmed, T. S.; Grubbs, R. H. Fast-Initiating, Ruthenium-based Catalysts for Improved Activity in Highly E-Selective Cross Metathesis. *J. Am. Chem. Soc.* **2017**, *139*, 1532−1537.

(10) Vougioukalakis, G. C.; Grubbs, R. H. Ruthenium-Based Olefin Metathesis Catalysts Coordinated with Unsymmetrical N-Heterocyclic Carbene Ligands: Synthesis, Structure, and Catalytic Activity. *Chem. - Eur. J.* **2008**, *14*, 7545−7556.

(11) Diver, S. T.; Griffiths, J. R. *Factors Affecting Initiation Rates*; Wiley: New York, 2014; Vol. *1*, Catalyst Development and Mechanism.

(12) The mechanism is associative for small alkenes.

(13) Gatti, M.; Vieille-Petit, L.; Luan, X.; Mariz, R.; Drinkel, E.; Linden, A.; Dorta, R. Impact of NHC Ligand Conformation and Solvent Concentration on the Ruthenium-Catalyzed Ring-Closing Metathesis Reaction. *J. Am. Chem. Soc.* **2009**, *131*, 9498−9499.

(14) (a) Ashworth, I. W.; Hillier, I. H.; Nelson, D. J.; Percy, J. M.; Vincent, M. A. What is the initiation step of the Grubbs-Hoveyda olefin metathesis catalyst? *Chem. Commun.* **2011**, *47*, 5428−5430. (b) Nunez-Zarur, F.; Solans-Monfort, X.; Rodriguez-Santiago, L.; Sodupe, M. Differences in the activation processes of phosphine-containing and Grubbs-Hoveyda-type alkene metathesis catalysts. *Organometallics* **2012**, *31*, 4203−4215. (c) Ashworth, I. W.; Hillier, I. H.; Nelson, D. J.; Percy, J. M.; Vincent, M. A. Olefin Metathesis by Grubbs−Hoveyda Complexes: Computational and Experimental Studies of the Mechanism and Substrate-Dependent Kinetics. *ACS Catal.* **2013**, *3*, 1929−1939.

(15) Vorfalt, T.; Wannowius, K.-J.; Plenio, H. Probing the Mechanism of Olefin Metathesis in Grubbs−Hoveyda and Grela Type Complexes. *Angew. Chem., Int. Ed.* **2010**, *49*, 5533−5536.

(16) Pump, E.; Leitgeb, A.; Kozłowska, A.; Torvisco, A.; Falivene, L.; Cavallo, L.; Grela, K.; Slugovc, C. Variation of the Sterical Properties of the N-Heterocyclic Carbene Coligand in Thermally Triggerable Ruthenium-Based Olefin Metathesis Precatalysts/Initiators. *Organometallics* **2015**, *34*, 5383−5392.

(17) Ritter, T.; Hejl, A.; Wenzel, A. G.; Funk, T. W.; Grubbs, R. H. A Standard System of Characterization for Olefin Metathesis Catalysts. *Organometallics* **2006**, *25*, 5740−5745.

(18) Nelson, D. J.; Queval, P.; Rouen, M.; Magrez, M.; Toupet, L.; Caijo, F.; Borré, E.; Laurent, I.; Crévisy, C.; Baslé, O.; Mauduit, M.; Percy, J. M. Synergic Effects Between N-Heterocyclic Carbene and Chelating Benzylidene−Ether Ligands Toward the Initiation Step of Hoveyda−Grubbs Type Ru Complexes. *ACS Catal.* **2013**, *3*, 259−264.

(19) Stewart, I. C.; Ung, T.; Pletnev, A. A.; Berlin, J. M.; Grubbs, R. H.; Schrodi, Y. Highly Efficient Ruthenium Catalysts for the Formation of Tetrasubstituted Olefins via Ring-Closing Metathesis. *Org. Lett.* **2007**, *9*, 1589−1592.

(20) Urbina-Blanco, C. A.; Leitgeb, A.; Slugovc, C.; Bantreil, X.; Clavier, H.; Slawin, A. M. Z.; Nolan, S. P. Olefin Metathesis Featuring Ruthenium Indenylidene Complexes with a Sterically Demanding NHC Ligand. *Chem. - Eur. J.* **2011**, *17*, 5045−5053.

DOI: 10.1021/acs.organomet.8b00041
Organometallics XXXX, XXX, XXX−XXX